

## Removal of amoxicillin from wastewater by adsorption onto activated carbon prepared from sunflower seed hulls

Sarmad A. Rashid<sup>a,\*</sup>, Tariq M. Naife<sup>a</sup>, Badoor M. Kurji<sup>b</sup>

<sup>a</sup>Department of Chemical Engineering, University of Baghdad, Baghdad, Iraq, Tel. +964 7709 808686;

emails: sermed.rashid@coeng.uobaghdad.edu.iq (S.A. Rashid), Tariq.mohammed@coeng.uobaghdad.edu.iq (T.M. Naife)

<sup>b</sup>Department of Chemical and Petrochemical Engineering, University of Anbar, Anbar, Iraq,

email: Bdoorm.kurji@uoanbar.edu.iq (B.M. Kurji)

Received 20 December 2021; Accepted 25 September 2022

### ABSTRACT

In this study, the potential of adsorption of amoxicillin antibiotic (AMOX) from aqueous solutions using prepared activated carbon (AC) was studied. The used AC was prepared from an inexpensive and available precursor (sunflower seed hulls (SSH)) and activated by potassium hydroxide (KOH). The prepared AC was examined for its ability to remove AMOX from aqueous contaminated solutions and characterized with the aid of N<sub>2</sub>-adsorption/desorption isotherm Brunauer–Emmett–Teller, scanning electron microscopy, energy-dispersive X-ray spectroscopy and Fourier-transform infrared. Zeta potential of the prepared activated carbon from sunflower seed hulls (SSHAC) were studied in relation to AMOX adsorption. The physical and chemical properties of SSHAC were analyzed and it showed successful preparation of SSHAC with a preferable surface area, micropores volume and average pore diameter of 928.706 m<sup>2</sup>/g, 0.565 cm<sup>3</sup>/g and 2.55 nm, respectively due to the hierarchical porosity of the prepared adsorbent. SSHAC exhibited a removal percentage of 95% for AMOX at a solution pH of 6, SSHAC dosage of 0.75 g/L and an initial AMOX amount of 50 mg/L. Equilibrium analysis were performed in a batch model within the range of 5–9 solution pH, 0.25–1.25 mg/mL SSHAC dosage and 50–250 mg/L AMOX initial concentration. The experimental data obtained were analyzed by Langmuir, Freundlich and Temkin isotherm models. The equilibrium data fitted well with the Langmuir model with a maximum AMOX adsorption capacity of 272.44 mg/g. Pseudo-first-order, pseudo-second-order and intraparticle diffusion models were utilized to examine the kinetic data obtained at various inlet AMOX concentrations. The kinetic experimental data were well fitted with the pseudo-first-order equation. A proposed adsorption mechanism by  $\pi$ - $\pi$  interactions were introduced. From the obtained results, SSHAC is recommended as a highly efficient adsorbent for removal of AMOX from aqueous solutions.

*Keywords:* Activated carbon; Adsorption; Amoxicillin; Sunflower seed hulls; Potassium hydroxide

### 1. Introduction

The presence of contaminants in wastewater represents one of the modern environmental threats and global challenges, which have to control and treatment [1]. This excites interesting of more research centers and environmental protection foundations around the world [2]. From these

pollutants, pharmaceuticals especially antibiotics which come from drugs factories, excrement of humans and animals, hospital effluents [3] and inefficient water treatment plants [4]. The existence of antibiotics in the surface water may leads to respiratory problems, skin irritation and can also cause cancer and cell mutation risk in human beings [5,6].

\* Corresponding author.

The studies showed that most of the antibiotics cannot be consumed and absorbed well from organisms [7]. Therefore, about 30%–90% of these pollutants reach and spread to the aquatic environment as a part of human and animals' excrement and urine [8]. The appearance of antibiotics in water causes toxicity for aquatic life for long time especially on algae and lower organisms even with very low concentrations. Antibiotics cause adverse effects on human and animals like sharp and chronic toxicity as well as emergence of multi resistant bacteria [9,10].

Amoxicillin (AMOX) is one of the antibiotics that widely used. It is from beta-lactam family and penicillin type. The mechanism of its activity is stopping and preventing of bacteria growth [11]. Consequently, it used to treat skin infections, pneumonia, ear and throat infections and more uses [12]. Furthermore, AMOX is classified within the list of essentially drugs reported by the World Health Organization as one of drugs with a big deal of activity and safely [13]. However, the studies proved that more than 80% of AMOX used for treating humans and animals, are excreted with urine within no more than 2 h after used and discharges into surface water [13].

The wastewater treatment plants are unable to remove contaminants especially antibiotics [11]. Therefore, several methods have been used to remove these contaminants. For example, catalytic degradation [14] ozonation [15], biodegradation [16] membrane filtration [17], photocatalytic degradation [18], photo-transformation [19], electrocoagulation [20], electrochemical [21], advanced oxidation [12], extraction [22] and adsorption [17]. Among these methods, it has been found that adsorption is one of the most effective techniques in the removal of antibiotics from aqueous solutions [23]. Both organic and inorganic materials can be removed by adsorption process even with very low amounts [24]. Adsorption is very simple method in operation and maintenance [25]. Also due to its lower initial operating cost and high efficiency for eliminating of antibiotics from contaminated wastewaters even with very low concentrated pollutants (less than 1 mg/L) [26,27]. Furthermore, the performance of adsorption depends on the efficient surface area and properties of adsorbent material used [28].

Activated carbon (AC) is one of the most effective adsorbents in removing of organic pollutants from wastewater because of its high adsorption capacity [29,30]. Its textural properties (surface area and pore volume) [31], mechanical strength, thermal stability [32], as well as efficient removal of contaminants may reach (in some cases) to 100% [33,34].

Sunflower seeds (SS) are one of the most significant oil seeds in the world with a global production of 416 million tons in the year 2013/2014 [35]. Universally, sunflowers are grown on about 24 million hectares, (National Sunflower Association, 2011) [36]. Every year a huge amount of sunflower seed hulls (SSH) is accumulated as a by-product of SS oil refining. In the last years, SSH was examined as an efficient, economic and renewable precursor for preparing highly porous ACs [37]. The high carbon content of SSH within the range of 41%–51%, make SSH an efficient precursor for carbonaceous materials [38].

Several researches have been carried out and proved that AC can be represented as an efficient adsorbent [39,40]. Different activators were used to activate the carbonized precursor SSH like NaOH, H<sub>3</sub>PO<sub>4</sub>, ZnCl<sub>2</sub> and CO<sub>2</sub>. So far, very little attention has been adopted to use KOH as an activator to prepare efficient, low cost and eco-friendly adsorbent. To the authors knowledge, this is the first study that deals with preparation of activated carbon from sunflower seed hulls (SSHAC) as an eco-friendly adsorbent from SSH using KOH as an activator.

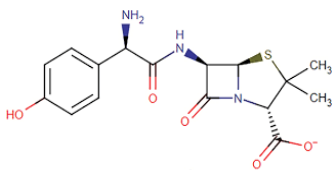
In this work, the potential and adsorption capacity of SSHAC in removing AMOX from aqueous solutions was investigated. The adsorption of AMOX was enhanced by increasing the diffusion inside the pores of adsorbent due to its hierarchical porosity. The SSHAC was characterized using surface area morphology, porosity and active groups. The impact of several factors such as initial pH of solution, dosage of adsorbent and initial adsorbate amount were investigated. Also the equilibrium isotherm and kinetic models were performed to understand the adsorption behavior.

## 2. Materials and methods

### 2.1. Materials

The chemicals used in this work include KOH, NaOH, HCl (BDH Limited Poole, England) and AMOX (Brawn Laboratories Limited, Faridabad-121001, Haryana, India). The chemical and physical properties of AMOX are shown in Table 1 [7,9]. The hulls of sunflower seeds (SSH) were provided by a local oil factory (Baghdad, Iraq). The SSH were cleaned with deionized water to remove impurities and dust, dried in an oven (Gallenkamp-Model No. IH-100, England) at 110°C for 24 h and allowed to cool to a room temperature. The dried hulls were crushed in a mill (LABSCO

Table 1  
Chemical and physical properties of AMOX [7,9]

Chemical symbol	Chemical structure	Molecular weight (g/mol)	Solubility in water (mg/L)	Melting point (°C)	Density, g/cm <sup>3</sup> (25°C)	pKa
C <sub>16</sub> H <sub>19</sub> N <sub>3</sub> O <sub>5</sub> S		365.4	3,430 at 20°C	194	320	2.68 7.49 9.63

D-6360/H, Germany) in order to get a particle size of 250–500  $\mu\text{m}$ .

## 2.2. Preparation and characterization of activated carbon

15 g of the dried precursor (SSH) were mixed very well with 50 mL of KOH solution as an activator with impregnation ratio of 0.5, 1 and 2 for 24 h at a room temperature. After that, all samples were fully dried at 110°C and kept in a desiccator. To carbonize the samples, a stainless steel reactor (10 cm height and 2.5 cm inside diameter) was used, it has a removable cover with a centric hole of 1.5 mm to allow the released gases to exit from the reactor. A furnace (Nabertherm N-20/H, Germany) was used to heat the samples at a heating rate of 10°C/min with various activation temperatures of 400°C, 600°C and 800°C and different activation times of 0.5, 1.5 and 2.5 h. After the activation under the specified conditions, the samples were removed from the furnace and allowed to cool to room temperature. Then, the samples were steeped with 0.1 M of HCl at a liquid to solid ratio of 10 mL/g for 24 h, filtered and washed with distilled water in order to make the pH of solution reach the value of 6.5–7. The samples were dried at 110°C for whole a day and weighed to find the product yield. Eventually, the samples were placed in tightly sealed containers. Eq. (1) represents the value of the yield of adsorbent which equal to the ratio of final amount of the product to the primary amount of the fully dried precursor [41].

$$\text{Yield}(\%) = \frac{W_f}{W_o} \times 100 \quad (1)$$

where  $W_f$  is the final weight of SSHAC product (g) and  $W_o$  is the weight of dried SSH (g).

The prepared SSHAC was characterized by  $\text{N}_2$ -adsorption/desorption isotherm Brunauer–Emmett–Teller (BET) at 77 K in order to evaluate the BET surface area, pore volume and average pore diameter of the prepared SSHAC [42] using a Thermo Finnigan, USA. The morphologies of different samples were analyzed via scanning electron microscopy (SEM) using a model Inspect S50, FEI Company, Netherlands. Also the energy-dispersive X-ray spectroscopy (EDX) was observed by XFlash 6110, Bruker Company, Germany. Fourier-transform infrared (FTIR) spectroscopy analysis was carried out by Shimadzu with scanning range of 4,000–400  $\text{cm}^{-1}$  to test the bonds between molecules by forming an infrared adsorption spectrum and to provide details about functional groups of the adsorbents. The results were recorded at a resolution of 4  $\text{cm}^{-1}$  [3]. The zeta potential (ZP) of the prepared SSHAC was evaluated as a relate to pH (using 0.1 M HCl or NaOH) by Zetasizer, UK.

## 2.3. Examination of the samples

The amount of AMOX in the aqueous solutions before and after adsorption performed using a single beam UV spectrophotometer (Shimadzu UV-160A, Japan) at a wave length of (284) nm. The obtained calibration curve was linear for the used concentration range in this research.

## 2.4. Adsorption isotherms

The equilibrium adsorption isotherms of AMOX adsorption onto prepared SSHAC were performed in a set of Erlenmeyer flasks (100 mL). Each flask contains 40 mL of AMOX solution with different initial concentrations (50–250 mg/L). Drops of 0.1 M HCl solution were added in order to adjust the pH of the solutions to 6. Then, 0.02 g of the prepared SSHAC with a particle size of 250  $\mu\text{m}$  was added to AMOX solutions and each sample was shaken at (120 rpm at 30°C) for 24 h to ensure reaching equilibrium. Then, the samples were filtered and analyzed using UV spectrophotometer at appropriate wave length of 284 nm. The removed amount of AMOX  $q_e$  (mg/g) and the removal percentage were calculated by the following equations [43,44]:

$$\text{Adsorption capacity } q_e = \frac{(C_o - C_e)V}{W} \quad (2)$$

$$\text{Removal percentage}(\%) = \frac{(C_o - C_e)}{C_o} \times 100 \quad (3)$$

where  $C_o$  and  $C_e$  are the inlet and equilibrium amounts of AMOX solution (mg/L), respectively.  $V$  is the volume of solution (L) and  $W$  is the weight of used adsorbent (g).

The investigation of kinetics studies was mainly similar to those of equilibrium adsorption isotherms. The samples were withdrawn at programmed time periods and the amounts of AMOX were similarly measured.

## 3. Results and discussion

### 3.1. Activated carbon yield and characteristics

The yield of prepared SSHAC according to Eq. (1) at activation temperature of 400°C, activation time of 1 h and impregnation ratio of 1 g/g was 52%. Zou et al. [26] reported 40% yield at 650°C activation temperature, 1 h activation time and 3 g/g impregnation ratio for SSHAC prepared from SSH by  $\text{ZnCl}_2$  activation. The high yield of this investigation may be related to the KOH activation at low temperature (400°C), which causes low burn-off or activation degree [45].

The morphology of SSH and SSHAC before and after the AMOX adsorption was obtained by SEM and is shown in Fig. 1. Fig. 1A shows smooth surface of SSH, while Fig. 1B shows the rougher surface with uniform pores distribution of SSHAC. This result is due to the evaporation of components during the burning at an isolated reactor [10,23]. Fig. 1C reveals that the pores of SSHAC were filled with AMOX molecules [5]. The EDX spectrum in Fig. 1D shows the expected components present in the prepared SSHAC [46].

FTIR spectrum of SSHAC has emphasized the presence of many important functional groups on the surface of SSHAC as shown in Fig. 2. The existence of a wide band within the range from 2,800 to 3,200  $\text{cm}^{-1}$  because of the presence of amine (N–H) and hydroxyl (O–H) extending vibration groups [12,47]. The band around 1,600  $\text{cm}^{-1}$  indicates the symmetric and asymmetric vibration mode C–H

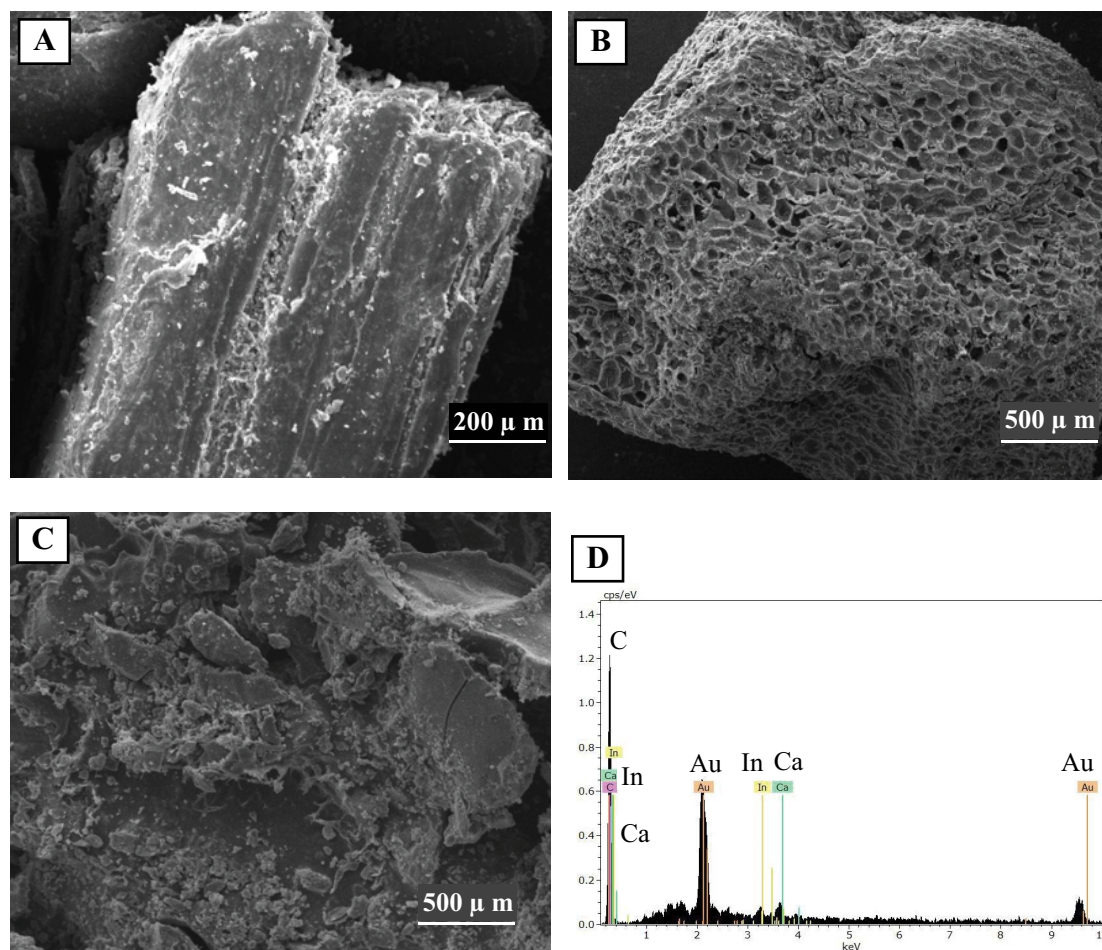


Fig. 1. SEM images of (A) SSH, (B) SSHAC before adsorption, (C) SSHAC after adsorption and (D) EDX spectrum.

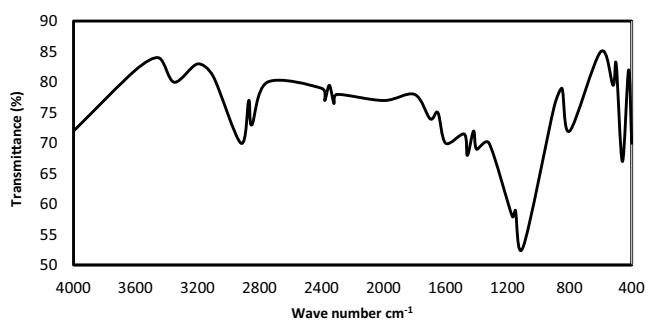


Fig. 2. FTIR of SSHAC.

group in alkane [48]. The peak at  $1,080\text{ cm}^{-1}$  is attributed to the existence of C=C poly aromatic vibration of the ACs [36]. The peaks around  $795\text{ cm}^{-1}$  clarify the appearance of a C=C bond which can be attributed to the activation with KOH and the active sites on the surface of adsorbent [49]. The wide band at  $400\text{--}600\text{ cm}^{-1}$  ( $462\text{ cm}^{-1}$ ) relates to in plane / out of plane vibration of vinyl group (=C-H), C-O and C-N bonds [50]. The prepared SSHAC consists essentially of an amorphous structure with different oxygen-containing functional groups. Such groups may have a deep and important

influence on the surface properties of ACs as well as their removal characteristics [33]. The BET surface area, micro-pore volume and average pore diameter of SSHAC were  $928.706\text{ m}^2/\text{g}$ ,  $0.565\text{ cm}^3/\text{g}$  and  $2.55\text{ nm}$ , respectively. The high SSHAC yield, large surface area, high pore volume furthermore the simplicity of activation procedure, the SSHAC prepared in this work can be considered as an economic adsorbent for large-scale wastewater treatment.

### 3.2. Zeta potential of SSHAC

The surface charge density of SSHAC was investigated by measuring zeta potential (ZP) which refers to the potential difference between the solid medium and the external static layer of liquid contact with surface of adsorbent. ZP is affected by many factors like the pH of solution and the conductivity of the dispersion medium [51]. ZP of SSHAC was measured at different values of pH (2–10). Fig. 3 shows the relationship between ZP and the dispersion solution pH. The curve clearly consists of two regions connected at a point of  $\text{pH}_{\text{IEP}}$  (isoelectric point) where ZP equal to zero, this point appears at pH of 6.5. The first region with positive values of ZP (pH of 2–6.5) is due to the presence of positive functional group ( $\text{H}^+$ ) which increases the adsorption

rate because of the protonation of these positive functional group [52], however, the second region of negative ZP (pH of 6.5–10) which indicate the existence and deprotonation of negative charge functional groups ( $\text{OH}^-$ ) causing a decrease in the adsorption rate [53].

### 3.3. Effect of initial pH of solution on the adsorption capacity

The uptake of AMOX by adsorption onto the prepared SSHAC, as a function of pH, is presented in Fig 4A. Different values of initial pH AMOX solution of 5, 6, 7, 8 and 9 were used to carry out experiments for batch of AMOX adsorption. Solutions of 0.1 M NaOH and HCl

were used to adjust the values of pH solution. A significant effect of initial pH of AMOX solution on AMOX adsorption was observed, the uptake rate of AMOX decreased from 82% to 30% with rising of pH, a similar behavior for AMOX adsorption onto AC prepared from reed has been noticed [18], the electrostatic interaction between AMOX and SSHAC with opposite charges was the reason of this behavior. SSHAC has a number of functional groups belong to acidic oxygen which decreased with the pH value increasing, that lead to occupy active sites. In general, the acceptable range of pH value of wastewater that could be discharge into surface water is 6–9 [17].

### 3.4. Effect of mass of activated carbon on the adsorption process

The impact of SSHAC dosage on the uptake of AMOX from synthesis aqueous solutions was investigated. Different dosage range 0.25, 0.5, 0.75, 1.00 and 1.25 g/L was performed with 40 mL volume of AMOX solution, at initial solution pH of 6 and 150 mg/L of initial AMOX concentration for 24 h with agitation speed of 120 rpm. The results are introduced in Fig. 4B, the removal efficiency % of SSHAC increased and reached asymptotic certain value with the increasing weight of SSHAC dosage, it was observed that the maximum AMOX removal efficiency was 85% at 0.75 mg/mL. This trend can be demonstrated by the availability of adsorption active sites with the increase of dosage of SSHAC. Furthermore, after a certain value of SSHAC

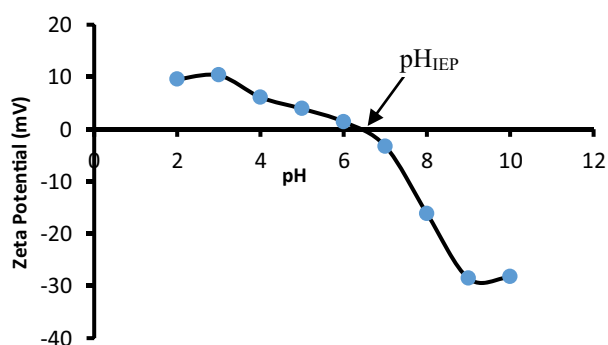


Fig. 3. Zeta potential of SSHAC surface.

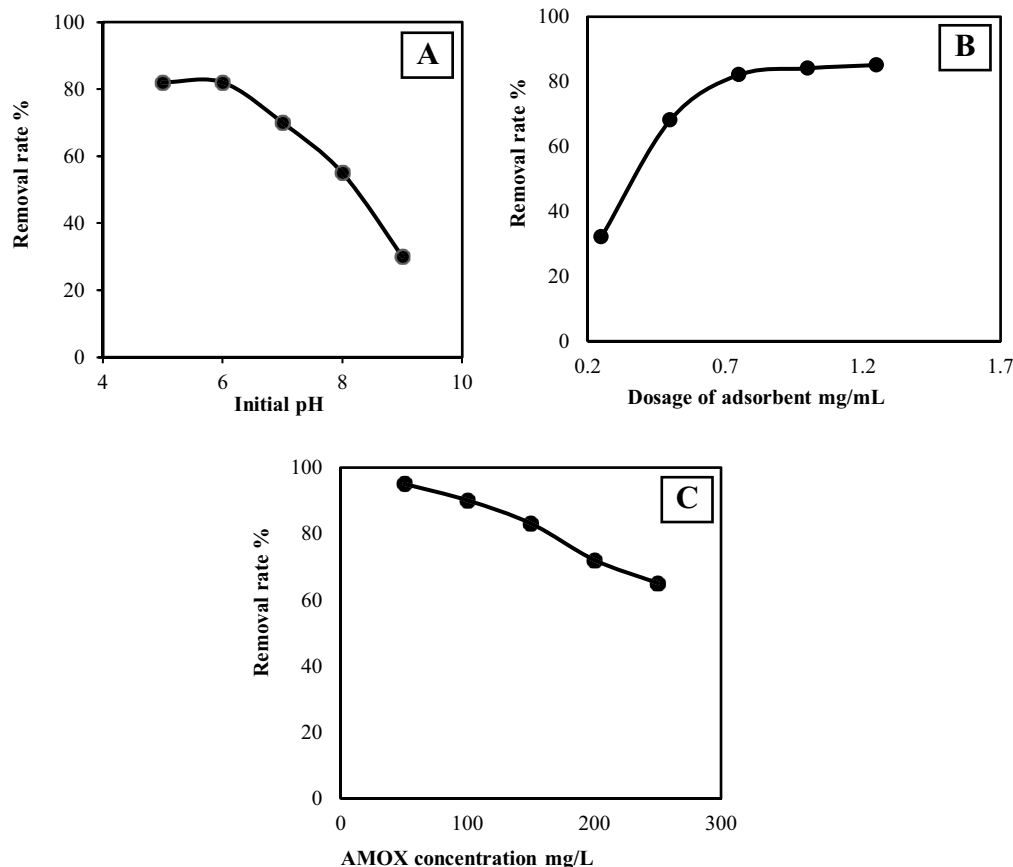


Fig. 4. (A) Effect of AMOX solution pH, (B) effect of SSHAC dosage, and (C) effect of initial AMOX concentration.



dosage 0.75, the extra rise in AC dosage never conducted to any increase in removal efficiency due to the reaching to equilibrium which mean there is no net mass transfer from adsorbate to adsorbent molecules. An identical behavior for ciprofloxacin and AMOX adsorption onto AC prepared from *Prosopis juliflora* was also reported [26].

3.5. Effect of initial AMOX concentration on adsorption process

The influence of initial AMOX concentration 50–250 mg/L on the removal efficiency of AMOX was tested at pH of 6 and AC dosage of 0.75 mg/mL, as presented in Fig. 4C. This figure showed that the AMOX removal efficiency was attained a maximum value of 95% at the initial concentration of 50 mg/L. Subsequently, the removal efficiency decreased with the increase of AMOX initial concentration until reach 65% at the initial concentration of 250 mg/L, this trend related to the identified availability of active uptake sites for increased amounts of AMOX particles [54]. On the other hand, the specific amount of SSHAC could not be able to provide enough surface area that required to remove all the amount of adsorbate. Similar trend was observed for removing AMOX antibiotic from water by adsorption onto AC [49].

Eventually, the results emphasized the effectiveness of the activation method that used to modify the SSHAC in order to improve its favorability for the removal of AMOX from pollutant waters.

3.6. Adsorption isotherm

Adsorption isotherms are essential relations to describe the behavior of adsorption systems at equilibrium state

[55]. The most common adsorption isotherms are the Langmuir [56], Freundlich [57], as well as, Temkin [58], these equations were applied to explain the relation between the adsorbed amount of AMOX and its amount in solutions at equilibrium.

The Langmuir model is appropriate for monolayer adsorption happened on a surface including limited number of similar sites [59]. The linear form of this model is given as:

$$\frac{C_e}{q_e} = \frac{1}{Q_0 b} + \frac{C_e}{Q_0} \tag{4}$$

where  $C_e$  (mg/L) refers the concentration at equilibrium of AMOX,  $q_e$  (mg/g) is the adsorbed quantity of AMOX per unit mass of SSHAC,  $Q_0$  is the Langmuir constant of the removal capacity and  $b$  is the Langmuir constant refer to the rate of adsorption. Fig. 5A shows a linear relationship of  $C_e/q_e$  vs.  $C_e$  representing the applicability of the Langmuir equation ( $R^2 = 0.99$ ). The applicability of this model confirms monolayer coverage of AMOX at the surface of SSHAC. Values of  $Q_0$  and  $b$  are estimated from the plot represented in Fig. 5A.

The Freundlich isotherm model can be expressed by the following equation [60]:

$$q_e = K_F C_e^{1/n} \tag{5}$$

where  $K_F$  (mg/g·(L/mg)<sup>1/n</sup>) and  $(1/n)$  refer to Freundlich constants which are relatively indicators of the adsorption capacity and the adsorption intensity, respectively [60]. Value of  $n < 1$  refers to weak absorption while value of  $n > 1$

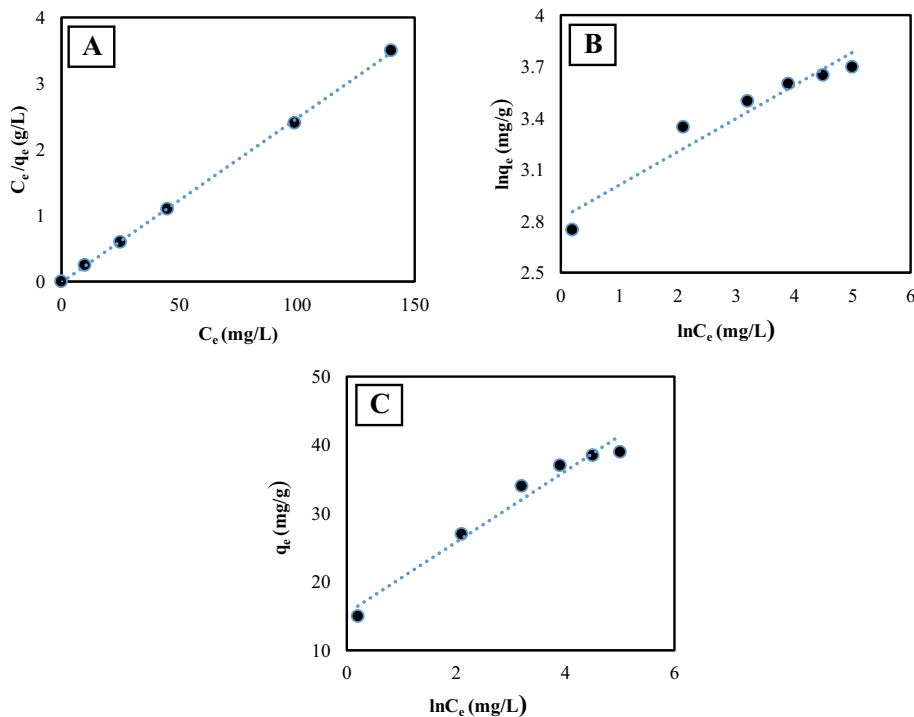


Fig. 5. Adsorption isotherm of AMOX uptake by SSHAC (A) Langmuir, (B) Freundlich, and (C) Temkin.

represents a favorable adsorption [61]. The linear form of Eq. (5) is represented by Eq. (6):

$$\ln q_e = \ln K_F + \left(\frac{1}{n}\right) \ln C_e \quad (6)$$

where represent a linear relationship having a slope of  $1/n$  as well as an intercept of  $\ln(K_F)$  when  $\ln(q_e)$  is plotted vs.  $\ln(C_e)$  as represented in Fig. 5B. The magnitude of  $n$  was reported to be 2.19, confirming that the adsorption process was preferable.

Temkin isotherm model considers the influences of indirect SSHAC/AMOX interactions on adsorption isotherms. The heat of process of all the particles in the layer would be reduced linearly with coverage because of SSHAC/AMOX interactions. Temkin isotherm can be written in linear form as follows [12]:

$$q_e = B \ln K_T + B \ln C_e \quad (7)$$

where  $K_T$  refers to Temkin constant and  $B = RT/b$ . Fig. 5C shows the relation between  $q_e$  and  $\ln C_e$ . The values of constants  $A$  and  $B$  as well as  $R^2$  are listed in Table 2.

Table 2  
Isotherms constants for AMOX adsorption onto SSHAC at 30°C

Models	Parameters	Values
Langmuir	$Q_o$ (mg/g)	272.44
	$b$ (L/mg)	0.21
	$R^2$	0.985
Freundlich	$K_F$ (mg/g·(L/mg) <sup>1/n</sup> )	33.78
	$n$	2.19
	$R^2$	0.84
Temkin	$A$ (L/g)	2.99
	$B$	27.67
	$R^2$	0.93

The correlation factor of Temkin model ( $R^2 = 0.93$ ) is less than that related to Langmuir model.

The parameters of the three models were calculated and listed in Table 2. By comparing the correlation coefficients  $R^2$ , it was found that  $R^2$  for Langmuir model (0.985) was higher than the other two models, therefore, this process was a good fitted with Langmuir isotherm model. An identical finding was obtained for the adsorption of AMOX on AC [62]. Table 2 shows that the estimated maximum monolayer adsorption capacity  $Q_o$  of AMOX on SSHAC was 272.44 mg/g. This roughly high adsorption capacity may be related to the effective high surface area 928.706 m<sup>2</sup>/g and to the uniform and homogenous distribution of active sites on the SSHAC surface having pores with hierarchical porosity. Table 2 also reveals that the magnitude of  $n$  for AMOX is more than one, that confirmed that the AMOX adsorption process is favorable. Adsorption isotherms of  $n$  value above one are categorized among L-type equilibrium isotherms and the process is chemical [63]. In this study, the value of  $1/n$  is lower than one, which means that the adsorption of AMOX on SSHAC at low AMOX amounts is better than that at high amounts. This indicates the adsorption is a chemical process [64]. Table 3 presents a comparison of adsorption capacity and specific surface area of AMOX adsorption in this work with those reported in the literatures. Eventually, it can be seen that the prepared SSHAC from an available and low cost precursor (SSH) is effective adsorbent which can be used for AMOX removal from pharmaceutical industries wastewater [34].

### 3.7. Adsorption kinetics

Kinetic models were applied to clarify the adsorption behavior of the AMOX-SSHAC system with unit time and to inspect parameters that affect the adsorption rate [68]. In this part, pseudo-first-order [69], pseudo-second-order [70], and intraparticle diffusion [71] were tested to examine the parameters influencing the adsorption rate of the AMOX uptake by SSHAC as adsorbent. The three adsorption kinetic equations can be expressed by Eqs. (8)–(10), respectively [68]:

Table 3  
Comparison between the maximum adsorption capacities and specific surface areas of AMOX onto AC prepared from different precursors with different activators at 30°C

Adsorbate (AC source)	Activator	Surface area (m <sup>2</sup> /g)	$Q_{max}$ (mg/g)	References
Sunflower seed hull	KOH	928.7	272.44	This study
Durian shell	CO <sub>2</sub>	917	142.714	[13]
Pomegranate peel	H <sub>3</sub> PO <sub>4</sub>	–	40.282	[12]
<i>Prosopis juliflora</i>	H <sub>3</sub> PO <sub>4</sub>	855	482.14	[65]
Reed	H <sub>3</sub> PO <sub>4</sub>	806.67	77.5	[18]
Cashew of Para	ZnCl <sub>2</sub>	1,457	451	[3]
Olive kernel	NaOH	2,188	238.1	[4,50]
Guava seeds	NaOH	2,573.6	570.45	[66]
Granular activated carbon	–	1,092.951	189.5	[11]
Olive biomass using furnace (ACF)	ZnCl <sub>2</sub>	1,742	237.02	[67]
Olive biomass using microwave (ACMW)	ZnCl <sub>2</sub>	1,742	166.96	[67]

$$\ln(q_e - q_t) = \ln q_e - k_1 t \tag{8}$$

$$\frac{t}{q_t} = \frac{1}{k_2 q_e^2} + \frac{1}{q_e} t \tag{9}$$

$$q_t = k_3 t^{1/2} + C \tag{10}$$

where  $q_e$  and  $q_t$  (mg/g) represent the adsorption capacity at equilibrium and at any time,  $t$  (min), respectively,  $k_1$  (1/min) refers to the rate constant of pseudo-first-order equation at equilibrium,  $k_2$  (g/mg·min) refers to the rate constant of pseudo-second-order equation at equilibrium,  $k_3$  (mg/g·min<sup>0.5</sup>) is the constant of intraparticle diffusion rate and  $C$  (mg/g) is the constant of adsorption that relevant to the thickness of boundary layer. On the other hand, in Eq. (8),  $q_e$  and  $q_t$  magnitudes represent the intercept on  $y$ -axis and the slope of the linear plot of  $\ln(q_e - q_t)$  against  $t$ ,

respectively. In Eq. (9)  $q_e$  and  $k_2$  magnitudes are found from the intercept and slope on  $y$ -axis of the linear plot of  $t/q_t$  vs.  $t$  [72]. In Eq. (10),  $q_t$  is the amount of adsorbate material (mg/g) at time  $t$ . Fig. 6 presents the pseudo-first-order kinetic, pseudo-second-order kinetic and intraparticle diffusion kinetic, respectively. Table 4 illustrates the factors of the three kinetic equations. The obtained results confirmed that pseudo-first-order model better represented the adsorption kinetics. This suggests is agreement with result introduced by [12] for the removal of AMOX by adsorption onto pomegranate peel. Furthermore, the rate constant of the pseudo-second-order equation ( $k_2$ ) has been reduced with the rise in AMOX amount as shows in Table 4. The reason of decreasing in velocity rate could be related to the existence of enough active sites in the structure of SSHAC at lower amounts of AMOX. Although, the rate of mass transfer was larger, it gradually decreased because of the reduction in active sites of SSHAC at large amounts of AMOX.

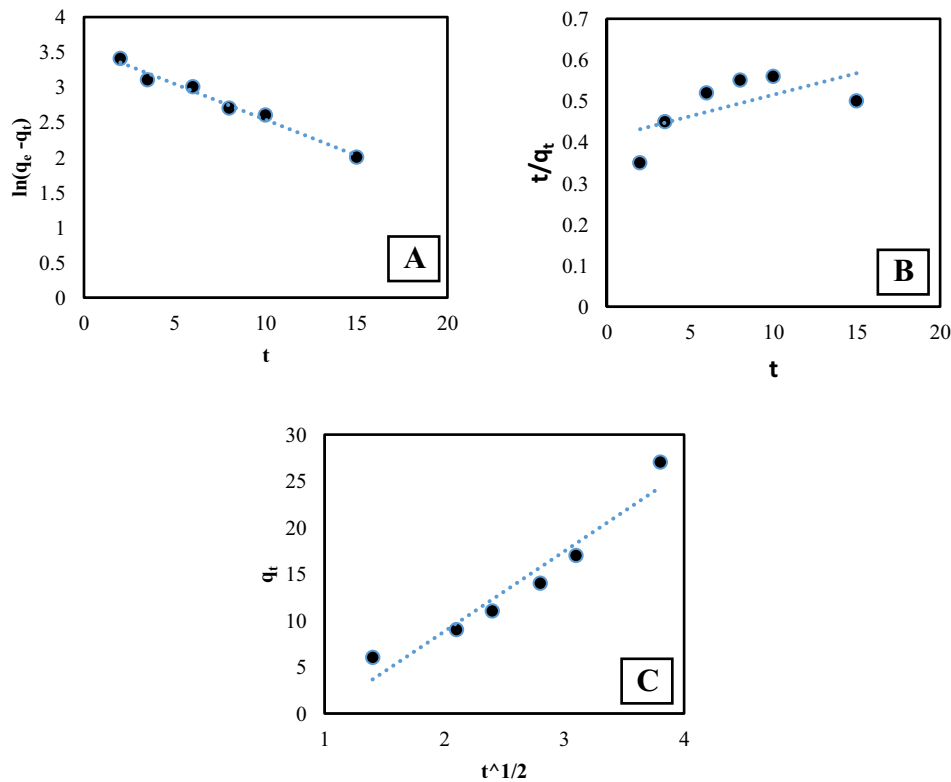


Fig. 6. Kinetic plots of AMOX uptake by SSHAC (A) pseudo-first-order, (B) pseudo-second-order, and (C) intraparticle diffusion.

Table 4  
Kinetic parameters for AMOX adsorption onto SSHAC

Pseudo-first-order model		Pseudo-second-order model		Intraparticle diffusion model	
Parameters	Values	Parameters	Values	Parameters	Values
$k_1$ (min <sup>-1</sup> )	0.078	$k_2$ (mg/g·min)	0.029	$k_3$ (mg/g·min <sup>0.5</sup> )	7.081
$q_e$ (mg/g)	37.156	$q_e$ (mg/g)	12.725	$C$	7.456
$R^2$	0.974	$R^2$	0.678	$R^2$	0.949



### 3.8. Adsorption mechanism

The main mechanisms for adsorption processes of antibiotics onto ACs can be attributed to the one of these mechanisms; electrostatic attraction or ion exchange (cation and anion attractions), hydrophobic interaction, hydrogen bonds, partition process, pore filling,  $\pi$ - $\pi$  interactions and surface precipitation [25,73]. According to the morphology, textural properties of SSHAC and the outcomes of the isotherm and kinetics studies, a reasonable mechanism can be predicted for AMOX adsorption onto SSHAC. The bindings of AMOX molecules with SSHAC prepared from SSH can be controlled by  $\pi$ - $\pi$  interactions (the binding occurring because of the bonds type  $\pi$  of both AMOX and SSHAC), polar groups attraction of oxygen-containing AMOX and the polar part of the SSHAC, and hydrogen bonds between the NH group of the AMOX molecules and the OH group of the SSHAC [67]. Furthermore, large number of AMOX particles can be attracted to the surface of SSHAC due to the accommodation properties such as high active surface area, micro pore volume and average pore diameter [47,74].

### 4. Conclusions

The present study demonstrated the feasibility of using sunflower seed hulls (SSH) as a low-cost precursor for preparing an efficient AC for the adsorption of antibiotics from contaminant solutions. From the results, the following conclusions are made: (1) a maximum removal percentage (95%) was attained at 6 pH value, 0.75 g/L SSHAC dosage and 50 mg/L AMOX initial concentration. (2) Potassium hydroxide (KOH) was successfully used as an activator in the chemical activation process as a result of studying the influence of impregnation ratio of KOH to SSH, activation temperature and activation time on the activation process of SSH. (3) The equilibrium data of AMOX adsorption onto SSHAC were well fitted with Langmuir model giving maximum adsorption capacity of 272.44 mg/g. (4) The kinetics of AMOX adsorption onto SSHAC followed the pseudo-first-order equation based on the values of  $R^2$  and  $q_e$ . (5) The fabricated adsorbent (SSHAC) revealed favorable morphological and structural characteristics (surface area and pore volume of SSHAC were 928.706 m<sup>2</sup>/g and 0.565 cm<sup>3</sup>/g, respectively). (6) The mechanism of AMOX adsorption onto SSHAC is controlled by  $\pi$ - $\pi$  stacking, electrostatic interaction, hydrophobic attraction, pore filling and hydrogen bonds. (7) The results confirmed that the prepared SSHAC adsorbent with high surface area and pore volume from an agriculture waste is favorable for applications controlling the water pollution and provided a very valuable, useful and economic material to the environment.

### References

- [1] S.M. Al-Jubouri, H.A. Al-Jendeel, S.A. Rashid, S. Al-Batty, Antibiotics adsorption from contaminated water by composites of ZSM-5 zeolite nanocrystals coated carbon, *J. Water Process Eng.*, 47 (2022) 102745, doi: 10.1016/j.jwpe.2022.102745.
- [2] J.J. Alvear-Daza, G.A. Pasquale, J.A. Rengifo-Herrera, G.P. Romanelli, L.R. Pizzio, Mesoporous activated carbon from sunflower shells modified with sulfonic acid groups as solid acid catalyst for itaconic acid esterification, *Catal. Today*, 372 (2021) 51–58.
- [3] D.R. Lima, E.C. Lima, C.S. Umpierrez, P.S. Thue, G.A. El-Chaghaby, R.S. da Silva, F.A. Pavan, S.L.P. Dias, C. Biron, Removal of amoxicillin from simulated hospital effluents by adsorption using activated carbons prepared from capsules of cashew of Para, *Environ. Sci. Pollut. Res.*, 26 (2019) 16396–16408.
- [4] J.M. Chaba, P.N. Nomngongo, Effective adsorptive removal of amoxicillin from aqueous solutions and wastewater samples using zinc oxide coated carbon nanofiber composite, *Emerging Contam.*, 5 (2019) 143–149.
- [5] D. Balarak, Z. Taheri, M.J. Shim, S.-M. Lee, C. Jeon, Adsorption kinetics and thermodynamics and equilibrium of ibuprofen from aqueous solutions by activated carbon prepared from *Lemna minor*, *Desal. Water Treat.*, 215 (2021) 183–193.
- [6] M.H. Alhassani, S.M. Al-Jubouri, H.A. Al-Jendeel, Stabilization of phenol trapped by agricultural waste: a study of the influence of ambient temperature on the adsorbed phenol, *Desal. Water Treat.*, 187 (2020) 266–276.
- [7] H. Azarpira, Y. Mahdavi, O. Khaleghi, D. Balarak, Thermodynamic studies on the removal of metronidazole antibiotic by multi-walled carbon nanotubes, *Der Pharm. Lett.*, 8 (2016) 107–113.
- [8] Z. Aksu, Ö. Tunç, Application of biosorption for penicillin G removal: comparison with activated carbon, *Process Biochem.*, 40 (2005) 831–847.
- [9] E. Kattel, B. Kaur, M. Trapido, N. Dulova, Persulfate-based photodegradation of a beta-lactam antibiotic amoxicillin in various water matrices, *Environ. Technol. (United Kingdom)*, 41 (2020) 202–210.
- [10] A.D. Khatibi, A.H. Mahvi, N. Mengelizadeh, D. Balarak, Adsorption-desorption of tetracycline onto molecularly imprinted polymer: isotherm, kinetics, and thermodynamics studies, *Desal. Water Treat.*, 230 (2021) 240–251.
- [11] E.K. Putra, R. Pranowo, J. Sunarso, N. Indraswati, S. Ismadji, Performance of activated carbon and bentonite for adsorption of amoxicillin from wastewater: mechanisms, isotherms and kinetics, *Water Res.*, 43 (2009) 2419–2430.
- [12] I. Ali, S. Afshinb, Y. Poureshgh, A. Azari, Y. Rashtbari, A. Feizizadeh, A. Hamzezadeh, M. Fazlzadeh, Green preparation of activated carbon from pomegranate peel coated with zero-valent iron nanoparticles (nZVI) and isotherm and kinetic studies of amoxicillin removal in water, *Environ. Sci. Pollut. Res.*, 27 (2020) 36732–36743.
- [13] A. Yazidi, M. Atrous, F. Edi Soetaredjo, L. Sellaoui, S. Ismadji, A. Erto, A. Bonilla-Petriciolet, G. Luiz Dotto, A. Ben Lamine, Adsorption of amoxicillin and tetracycline on activated carbon prepared from durian shell in single and binary systems: experimental study and modeling analysis, *Chem. Eng. J.*, 379 (2020) 122320, doi: 10.1016/j.cej.2019.122320.
- [14] R. Andreatti, M. Canterino, R. Marotta, N. Paxeus, Antibiotic removal from wastewaters: the ozonation of amoxicillin, *J. Hazard. Mater.*, 122 (2005) 243–250.
- [15] I.A. Balcioglu, M. Ötker, Treatment of pharmaceutical wastewater containing antibiotics by O<sub>3</sub> and O<sub>3</sub>/H<sub>2</sub>O<sub>2</sub> processes, *Chemosphere*, 50 (2003) 85–95.
- [16] S.-z. Li, X.-y. Li, D.-z. Wang, Membrane (RO-UF) filtration for antibiotic wastewater treatment and recovery of antibiotics, *Sep. Purif. Technol.*, 34 (2004) 109–114.
- [17] W.T. Mohammed, S.A. Rashid, Phosphorus removal from wastewater using oven-dried alum sludge, *Int. J. Chem. Eng.*, 2012 (2012) 125296, doi: 10.1155/2012/125296.
- [18] Z. Shang, Z. Hu, L. Huang, Z. Guo, H. Liu, C. Zhang, Removal of amoxicillin from aqueous solution by zinc acetate modified activated carbon derived from reed, *Powder Technol.*, 368 (2020) 178–189.
- [19] D. Balarak, A.H. Mahvi, M.J. Shim, S.M. Lee, Adsorption of ciprofloxacin from aqueous solution onto synthesized NiO: isotherm, kinetic and thermodynamic studies, *Desal. Water Treat.*, 212 (2021) 390–400.
- [20] F.Y. Aljaber, W.T. Mohammed, Effecting of pH parameter on simulated wastewater treatment using electrocoagulation method, *J. Eng.*, 24 (2018) 73–88.
- [21] G.A.M. Ali, O.A. Habeeb, H. Algarni, K.F. Chong, CaO impregnated highly porous honeycomb activated carbon from

- agriculture waste: symmetrical supercapacitor study, *J. Mater. Sci.*, 54 (2019) 683–692.
- [22] K.M. Abed, B.M. Kurji, S.A. Rashid, B.A. Abdulmajeed, Kinetics and thermodynamics of peppermint oil extraction from peppermint leaves, *Iraqi J. Chem. Pet. Eng.*, 20 (2019) 1–6.
- [23] D. Balarak, M. Baniyasi, S.M. Lee, M.J. Shim, Ciprofloxacin adsorption onto *Azolla filiculoides* activated carbon from aqueous solutions, *Desal. Water Treat.*, 218 (2021) 444–453.
- [24] S.A. Rashid, Increasing of naphthenes content in naphtha by using Y and zeolite prepared from Iraqi kaolin, *J. Eng.*, 20 (2014) 35–49.
- [25] H. Sadegh, G.A.M. Ali, A.S.H. Makhlof, K.F. Chong, N.S. Alharbi, S. Agarwal, V.K. Gupta, MWCNTs-Fe<sub>3</sub>O<sub>4</sub> nanocomposite for Hg(II) high adsorption efficiency, *J. Mol. Liq.*, 258 (2018) 345–353.
- [26] Z. Zou, Y. Tang, C. Jiang, J. Zhang, Efficient adsorption of Cr(VI) on sunflower seed hull derived porous carbon, *J. Environ. Chem. Eng.*, 3 (2015) 898–905.
- [27] H. Wang, J. Xu, X. Liu, L. Sheng, Preparation of straw activated carbon and its application in wastewater treatment: a review, *J. Cleaner Prod.*, 283 (2021) 124671, doi: 10.1016/j.jclepro.2020.124671.
- [28] B.D. Radhi, W.T. Mohammed, Novel nanocomposite adsorbent for desulfurization of 4,6-dimethylbenzothiophene from model fuel, *Mater. Today: Proc.*, 42 (2021) 2880–2886.
- [29] N.M. Hadi, S.A. Rashid, S. Abdalreda, Deep desulfurization of diesel fuel by guard bed adsorption of activated carbon and locally prepared Cu-Y zeolite, *J. Eng.*, 20 (2014) 146–159.
- [30] O.A. Habeeb, K. Ramesh, G.A.M. Ali, R. bin M. Yunus, Low-cost and eco-friendly activated carbon from modified palm kernel shell for hydrogen sulfide removal from wastewater: adsorption and kinetic studies, *Desal. Water Treat.*, 84 (2017) 205–214.
- [31] F.M. Kasperiski, E.C. Lima, C.S. Umpierrez, G.S. dos Reis, P.S. Thue, D.R. Lima, S.L.P. Dias, C. Saucier, J.B. da Janaina, Production of porous activated carbons from *Caesalpinia ferrea* seed pod wastes: highly efficient removal of captopril from aqueous solutions, *J. Cleaner Prod.*, 197 (2018) 919–929.
- [32] M.R. Cunha, E.C. Lima, N.F.G.M. Cimirro, P.S. Thue, S.L.P. Dias, M.A. Gelesky, G.L. Dotto, G.S. dos Reis, F.A. Pavan, Conversion of *Eragrostis plana* Nees leaves to activated carbon by microwave-assisted pyrolysis for the removal of organic emerging contaminants from aqueous solutions, *Environ. Sci. Pollut. Res.*, 25 (2018) 23315–23327.
- [33] A. Bahirai, J. Behin, Effect of citric acid and sodium chloride on characteristics of sunflower seed shell-derived activated carbon, *Chem. Eng. Technol.*, 44 (2021) 1604–1617.
- [34] R.M.Y. Omar Abed Habeeb, R. Kanthasamy, G.A.M. Ali, Application of response surface methodology for optimization of palm kernel shell activated carbon preparation factors for removal of H<sub>2</sub>S from industrial wastewater, *J. Teknol.*, 7 (2017) 1–10.
- [35] Z. Zou, Y. Tang, C. Jiang, J. Zhang, Efficient adsorption of Cr(VI) on sun flower seed hull derived porous carbon, *J. Environ. Chem. Eng.*, 3 (2015) 898–905.
- [36] K.Y. Foo, B.H. Hameed, Preparation and characterization of activated carbon from sunflower seed oil residue via microwave assisted K<sub>2</sub>CO<sub>3</sub> activation, *Bioresour. Technol.*, 102 (2011) 9794–9799.
- [37] X. Li, W. Xing, S. Zhuo, J. Zhou, F. Li, S.Z. Qiao, G.Q. Lu, Preparation of capacitor's electrode from sunflower seed shell, *Bioresour. Technol.*, 102 (2011) 1118–1123.
- [38] Y. Li, H. Shi, C. Liang, K. Yu, Turning waste into treasure: biomass carbon derived from sunflower seed husks used as anode for lithium-ion batteries, *Ionics (Kiel)*, 27 (2021) 1025–1039.
- [39] M. Yilmaz, T.J. Al-Musawi, M. Khodadadi Saloot, A.D. Khatibi, M. Baniyasi, D. Balarak, Synthesis of activated carbon from *Lemma minor* plant and magnetized with iron(III) oxide magnetic nanoparticles and its application in removal of ciprofloxacin, *Biomass Convers. Biorefin.*, (2022), doi: 10.1007/s13399-021-02279-y.
- [40] A.H. Omar, K. Ramesh, A.M.A. Goma, B.M.Y. Rosli, Experimental design technique on removal of hydrogen sulfide using CaO-eggshells dispersed onto palm kernel shell activated carbon: experiment, optimization, equilibrium and kinetic studies, *J. Wuhan Univ. Technol. Mater. Sci. Ed.*, 32 (2017) 305–320.
- [41] S.K. Theydan, M.J. Ahmed, Adsorption of methylene blue onto biomass-based activated carbon by FeCl<sub>3</sub> activation: equilibrium, kinetics, and thermodynamic studies, *J. Anal. Appl. Pyrolysis*, 97 (2012) 116–122.
- [42] S.A.S. Kamel, H.A. Al-Jendeel, W.T. Mohammed, Preparation of solid-super acidic catalyst with improvement physical properties, *Mater. Sci. Forum*, 1039 (2021) 313–325.
- [43] Z. Lin, X. Weng, G. Owens, Z. Chen, Simultaneous removal of Pb(II) and rifampicin from wastewater by iron nanoparticles synthesized by a tea extract, *J. Cleaner Prod.*, 242 (2020) 118476, doi: 10.1016/j.jclepro.2019.118476.
- [44] A. Azari, A. Babaei, R. Rezaei-kalantary, A. Esrafil, M. Moazzen, B. Kakavandi, M. Sciences, Nitrate removal from aqueous solution using carbon nanotubes magnetized by nano zero-valent iron, *J. Maz. Univ. Med. Sci.*, 23 (2014) 15–27.
- [45] M.J. Ahmed, S.K. Dhedan, Equilibrium isotherms and kinetics modeling of methylene blue adsorption on agricultural waste-based activated carbons, *Fluid Phase Equilib.*, 317 (2012) 9–14.
- [46] T.J. Al-Musawi, A.H. Mahvi, A.D. Khatibi, D. Balarak, Effective adsorption of ciprofloxacin antibiotic using powdered activated carbon magnetized by iron(III) oxide magnetic nanoparticles, *J. Porous Mater.*, 28 (2021) 835–852.
- [47] H.H. Abdel Ghafar, G.A.M. Ali, O.A. Fouad, S.A. Makhlof, Enhancement of adsorption efficiency of methylene blue on Co<sub>3</sub>O<sub>4</sub>/SiO<sub>2</sub> nanocomposite, *Desal. Water Treat.*, 53 (2015) 2980–2989.
- [48] M. Arshadi, M.K. Abdolmaleki, F. Mousavinia, S. Foroughifard, A. Karimzadeh, Nano modification of NZVI with an aquatic plant *Azolla filiculoides* to remove Pb(II) and Hg(II) from water: aging time and mechanism study, *J. Colloid Interface Sci.*, 486 (2017) 296–308.
- [49] G. Moussavi, A. Alahabadi, K. Yaghmaei, M. Eskandari, Preparation, characterization and adsorption potential of the NH<sub>4</sub>Cl-induced activated carbon for the removal of amoxicillin antibiotic from water, *Chem. Eng. J.*, 217 (2013) 119–128.
- [50] K. Jafari, M. Heidari, O. Rahmania, Wastewater treatment for amoxicillin removal using magnetic adsorbent synthesized by ultrasound process, *Ultrason. Sonochem.*, 45 (2018) 248–256.
- [51] A. Vafaei, A.M. Ghaedi, Z. Avazzadeh, V. Kiarostami, S. Agarwal, V.K. Gupta, Removal of hydrochlorothiazide from molecular liquids using carbon nanotubes: radial basis function neural network modeling and culture algorithm optimization, *J. Mol. Liq.*, 324 (2021) 114766, doi: 10.1016/j.molliq.2020.114766.
- [52] S.-x. Zha, Y. Zhou, X. Jin, Z. Chen, The removal of amoxicillin from wastewater using organobentonite, *J. Environ. Manage.*, 129 (2013) 569–576.
- [53] K.-H. Park, C.-H. Lee, S.-K. Ryu, X. Yang, Zeta-potentials of oxygen and nitrogen enriched activated carbons for removal of copper ion, *Carbon Lett.*, 8 (2007) 321–325.
- [54] M.J. Ahmed, S.K. Theydan, Adsorption of cephalixin onto activated carbons from *Albizia lebeck* seed pods by microwave-induced KOH and K<sub>2</sub>CO<sub>3</sub> activations, *Chem. Eng. J.*, 211–212 (2012) 200–207.
- [55] O.A. Habeeb, K. Ramesh, G.A.M. Ali, R. Bin M. Yunus, Isothermal modelling based experimental study of dissolved hydrogen sulfide adsorption from waste water using eggshell based activated carbon, *Malaysian J. Anal. Sci.*, 21 (2017) 334–345.
- [56] I. Langmuir, The constitution and fundamental properties of solids and liquids. Part I. Solids, *J. Am. Chem. Soc.*, 38 (1916) 2221–2295.
- [57] H. Freundlich, Über die Adsorption in Lösungen, *Zeitschrift Für Phys. Chemie.*, 57U (1907) 385–470.
- [58] M.I. Temkin, Kinetics of ammonia synthesis on promoted iron catalysts, *Acta Physiochim. URSS*, 12 (1940) 327–356.

- [59] K.R. Hall, L.C. Eagleton, A. Acrivos, T. Vermeulen, Pore- and solid-diffusion kinetics in fixed-bed adsorption under constant-pattern conditions, *Ind. Eng. Chem. Fundam.*, 5 (1996) 212–223.
- [60] B.H. Hameed, A.A. Rahman, Removal of phenol from aqueous solutions by adsorption onto activated carbon prepared from biomass material, *J. Hazard. Mater.*, 160 (2008) 576–581.
- [61] A. Azari, M. Salari, M.H. Dehghani, M. Alimohammadi, H. Ghaffari, K. Sharafi, N. Shariatifar, M. Baziar, Efficiency of magnetized graphene oxide nanoparticles in removal of 2,4-dichlorophenol from aqueous solution, *J. Maz. Univ. Med. Sci.*, 26 (2017) 265–281.
- [62] Z. Hu, M.P. Srinivasan, Preparation of high-surface-area activated carbons from coconut shell, *Microporous Mesoporous Mater.*, 27 (1999) 11–18.
- [63] M. Salari, M.H. Dehghani, A. Azari, M.D. Motevalli, A. Shabanloo, I. Ali, High performance removal of phenol from aqueous solution by magnetic chitosan based on response surface methodology and genetic algorithm, *J. Mol. Liq.*, 285 (2019) 146–157.
- [64] R. Khosravi, H. Hossini, M. Heidari, M. Fazlzadeh, H. Biglari, A. Taghizadeh, B. Barikbin, Electrochemical decolorization of reactive dye from synthetic wastewater by mono-polar aluminum electrodes system, *Int. J. Electrochem. Sci.*, 12 (2017) 4745–4755.
- [65] A. Chandrasekaran, C. Patra, S. Narayanasamy, S. Subbiah, Adsorptive removal of ciprofloxacin and amoxicillin from single and binary aqueous systems using acid-activated carbon from *Prosopis juliflora*, *Environ. Res.*, 188 (2020) 109825, doi: 10.1016/j.envres.2020.109825.
- [66] O. Pezoti, A.L. Cazetta, K.C. Bedin, L.S. Souza, A.C. Martins, T.L. Silva, O.O. Santos Júnior, J.V. Visentainer, V.C. Almeida, NaOH-activated carbon of high surface area produced from guava seeds as a high-efficiency adsorbent for amoxicillin removal: kinetic, isotherm and thermodynamic studies, *Chem. Eng. J.*, 288 (2016) 778–788.
- [67] D.L.C. Rodrigues, F.M. Machado, A.G. Osório, C.F. de Azevedo, E.C. Lima, R.S. da Silva, D.R. Lima, F.M. Gonçalves, Adsorption of amoxicillin onto high surface area-activated carbons based on olive biomass: kinetic and equilibrium studies, *Environ. Sci. Pollut. Res.*, 27 (2020) 41394–41404.
- [68] K. Sharafi, M. Pirsaeheb, R. Davoodi, H.R. Ghaffari, M. Fazlzadeh, M. Karimaei, M. Miri, K. Dindarlo, A. Azari, H. Arfaenia, Quantitative microbial risk assessment of giardia cyst and ascaris egg in effluent of wastewater treatment plants used for agriculture irrigation – a case study, *Desal. Water Treat.*, 80 (2017) 142–148.
- [69] S. Lagergreen, B. Svenska, Zur Theorie der sogenannten Adsorption gelöster Stoffe, *Zeitschr f Chem und Ind der Kolloide*, 15 (1907), doi: 10.1007/BF01501332.
- [70] Y.S. Ho, G. McKay, Pseudo-second-order model for sorption processes, *Process Biochem.*, 34 (1999) 451–465.
- [71] W.J. Weber, J.C. Morris, Kinetics of adsorption on carbon from solution, *J. Sanit. Eng. Div.*, 89 (1963) 31–59.
- [72] O.A. Habeeb, K. Ramesh, G.A.M. Ali, R. Bin M. Yunus, Isotherm, kinetic and thermodynamic of Reactive Blue 5 (RB5) dye adsorption using Fe<sub>3</sub>O<sub>4</sub> nanoparticles and activated carbon magnetic composite, *J. Color Sci. Technol.*, 7 (2013) 237–248.
- [73] M.B. Ahmed, J.L. Zhou, H.H. Ngo, W. Guo, Adsorptive removal of antibiotics from water and wastewater: progress and challenges, *Sci. Total Environ.*, 532 (2015) 112–126.
- [74] P. Pachauri, R. Falwariya, S. Vyas, M. Maheshwari, R.K. Vyas, A.B. Gupta, Removal of amoxicillin in wastewater using adsorption by powdered and granular activated carbon and oxidation with hydrogen peroxide, *Nat. Environ. Pollut. Technol.*, 8 (2009) 481–488.